**NURETH14-513** 

## PATHS: A Steady State Two-Phase Thermal Hydraulic Solver for PARCS Depletion

Benjamin Collins<sup>1</sup>, Linsen Li<sup>2</sup>, Dean Wang<sup>3</sup>, Shane Stimpson<sup>1</sup>, Daniel Jabaay<sup>1</sup>, Andrew Ward<sup>1</sup>, Yunlin Xu<sup>1</sup>, Thomas Downar<sup>1</sup>

University of Michigan, Ann Arbor, MI
 Tsinghua University, Beijing, China
 Oak Ridge National Laboratory, Oak Ridge, TN

### **Abstract**

The PATHS code was developed to solve the steady state two-phase thermal-hydraulic equations for a Boiling Water Reactor (BWR) and to provide thermal-hydraulic feedback for BWR depletion calculations with the neutronics code PARCS. The PARCS code is coupled to RELAP5 and TRACE which are normally used to solve for the thermal hydraulic state for BWR applications. However, systems codes were developed primarily for transient analysis and it can be computationally expensive to perform null transients to achieve the steady-state for the many channel problems required for practical BWR depletion analysis. For steady state analysis of the reactor, it is much more efficient to use a lower order two phase solution methodology. The low order methodology improves the runtime without major compromises in the fluid density and temperature distributions that are important for depletion analysis. In the PATHS code, the drift flux model is used with the EPRI void model. PATHS results were compared to TRACE for fixed power computations at various powers and flow rates. Coupled PATHS/PARCS calculations were then validated using depletion data from cycles 1 and 2 of the Peach Bottom II BWR.

#### 1. Introduction

The accurate analysis of Boiling Water Reactors requires the use of coupled neutronics and thermal hydraulics because of the strong dependency between power and void fraction. The standard modelling methodology for PARCS when analysing BWR systems is to utilize a one dimensional systems thermal-hydraulics code such as TRACE or RELAP5 [1]. In order to accurately perform steady state and depletion calculations it is important to model each channel in the reactor. However, the use of TRACE and RELAP to model more than 700 parallel channels requires a considerable computational effort. Systems analysis codes such as TRACE and RELAP5 were not developed for depletion calculations and it is computationally expensive to perform null transients to achieve the steady-state for the many channel problems required for practical BWR depletion analysis. For steady state analysis of the reactor it is much more efficient to use a lower order two phase solution methodology to improve the runtime without major compromises in the fluid density and temperature distributions that are important for depletion analysis. Other neutronics codes such as NESTLE and SIMULATE have developed internal thermal hydraulic solvers to provide these feedback effects [2].

In this paper the PATHS methodology is presented including the final form of the discrete equations, the constitutive relationships used, and the solution procedure for the standalone and coupled solution procedures. PATHS is benchmarked against TRACE for a single heated channel. Both PATHS and TRACE are run for a series of power and flow conditions and compared to data provided in the EPRI report [6]. A coupled full core calculation is then performed using both

TRACE and PATHS coupled to PARCS with CASMO-4 cross-sections and compared with TIP data from the Peach Bottom BWR. Finally, PARCS and PATHS are validated using data from Peach Bottom Cycles 1 and 2 depletion.

## 2. PATHS Methodology

The PATHS methodology is based on the two fluid model developed by Ishii [3], averaged to consider the mixture instead of two separate cases. The finite volume method is applied and the equations are cast into a face-based scheme. Since the control volume is set to include the entire cross-sectional area in a channel, the equations are reduced to a one dimensional flow with heat fluxes and stress terms coming from the boundary. The void fraction and drift velocity are introduced through constitutive relationships instead of a fourth field equation that would normally show up in the drift-flux model.

### 2.1 Discrete Equations

The final form of the discrete equations for continuity, momentum, and energy are shown in equations (1), (2), and (3) respectively.

$$(\rho A)_n u_n - (\rho A)_c u_s = 0 \tag{1}$$

$$\left(\rho u^* \hat{A}\right)_n u_n - \left(\rho u^* \check{A}\right)_s u_s + A_n P_n - A_s P_s = -\left(\frac{\alpha}{1 - \alpha} \frac{\rho_l \rho_g}{\rho} V_{gj}^2 A\right)_n + \left(\frac{\alpha}{1 - \alpha} \frac{\rho_l \rho_g}{\rho} V_{gj}^2 A\right)_s - \overline{\rho} g \Delta V$$

$$\hat{A}_n = \left(A_n + \frac{\Phi_{2\Phi}}{2} \left(\frac{f}{D_H} + \frac{K_{loss}}{\Delta z}\right) \Delta V\right) \qquad \qquad \check{A}_s = \left(A_s - \frac{\Phi_{2\Phi}}{2} \left(\frac{f}{D_H} + \frac{K_{loss}}{\Delta z}\right) \Delta V\right)$$
(2)

$$(\rho u^* A)_n h_n - (\rho u^* A)_s h_s = q^* \Delta V - \left(\alpha \frac{\rho_l \rho_g}{\rho} \Delta h_f V_{gl} A\right)_n + \left(\alpha \frac{\rho_l \rho_g}{\rho} \Delta h_f V_{gl} A\right)_s + \left(\overline{u} + \frac{\overline{\alpha} (\rho_l - \rho_g)}{\overline{\rho}} \overline{V_{gl}}\right) (P_n^* A_n - P_s^* A_s)$$
(3)

The n and s subscripts represent the north and south face of the node respectively following the notation of Patankar [4].

# 2.2 Constitutive Relationships

Several constitutive relations are needed to specify both thermal and mechanical properties of the flow. These include the void fraction, drift velocity, density, friction losses, latent heat of vaporization, and heat source. Some of these parameters are interdependent such as the density and drift velocity which are functions of the void fraction. The interdependencies are resolved using an iterative method. The calculation of density is performed using equations of state. In the subcooled region, the density is a function of enthalpy and pressure. In the saturated region, the fluid and gas densities are solely a function of pressure and the mixture density is a weighted sum of these densities. All thermophysical properties are based on the IAPWS-IF97 formulation [5].

The void fraction is a relationship between the flow of liquid and gas as well as the relative velocity between the two phases. These relationships are also dependent on flow regime. This model begins with the general equation for the void fraction.

$$\alpha = \frac{x}{C_o \left( x + \frac{\rho_g}{\rho_l} (1 - x) \right) + \frac{\rho_g V_{gj}}{\rho u}}$$
(4)

The distribution parameter  $C_o$  and drift velocity  $V_{gj}$  are determined through the use of constitutive relationships. Appendix A describes the different relationships employed in PATHS.

$$C_{0} = f(\alpha, P, h, D_{h}, u)$$

$$V_{oi} = f(\alpha, P, h, D_{h}, u)$$
(5)

Other constitutive relationships are needed to model subcooled boiling, friction factors, and two phase friction multipliers. The subcooled boiling model is based on the EPRI model [6] and adjusts the quality used in equation (4) to account for subcooled boiling. The Darcy friction factors are based on an approximate Moody relationship and the two-phase pressure drop is based on homogenous two phase friction multipliers.

## 3. PATHS Verification Study

The reference design specifications for the Peach Bottom Unit 2 (PB2) Nuclear Power Plant (NPP) are based on information provided in the EPRI report [7]. The PB2 NPP is a GE-designed BWR/4 with a rated thermal power of 3,293 MW, a rated core flow of 12,915 kg/s (102.5 Mlb/hr), a rated steam flow of 1,685 kg/s (13.37 Mlb/hr), and a turbine inlet pressure of 6.65 MPa (965 psia). The nuclear steam supply system (NSSS) has turbine-driven feed pumps and a two-loop M-G driven recirculation system feeding a total of 20 jet-pumps. This system contains a total of four steam lines; each has a flow-limiting nozzle, main steam isolation valves (MSIVs), safety relief valves (SRVs), and a turbine stop valve (TSV). The steam by-pass system consists of nine bypass valves (BPVs) mounted on a common header, which is connected to each of the four steam lines.

The reactor core consists of 764 fuel bundles with an active fuel length of 365.76 cm (12 ft) in the core region. The cycle 1 core is loaded entirely with  $7 \times 7$  fuel bundles with pitch/outer diameter (P/D) = 1.87452 cm / 1.43002 cm (0.738 in / 0.563 in). Cycle 2 fuel bundles consist of 576 of the original  $7 \times 7$  fuel assemblies, and 188 partial reload  $8 \times 8$  fuel bundles with P/D = 1.62560 cm / 1.25222 cm (0.640 in / 0.493 in). Additionally, the core region includes 185 control rods (CRs). For

the reactor protection system (RPS), the control systems for reactor pressure, recirculation flow, and feedwater flow and reactor water level are the same as commonly used in BWR reactors of this design. Some of the core data for PB2 is summarized in Table 1.

**Table 1: Peach Bottom 2 Core Data** 

Total Fuel Assemblies	764
Control Elements	185
Average Linear Heat Rate, kw/ft	7.037
Core Lattice Pitch, cm (in)	365.76 (12.0)
Water/UO2 Ratio (Cold)	2.51
Total Weight of U in Core (ST)	159.2
Number of In-Core Flux Monitors	43

Peach Bottom 2 startup testing was initiated in March, 1974. The power, flow, subcooling, and control rod notches inserted were recorded from the P1 edits of the process computer for each day of operation. A sample dataset for the month of April is shown in Figure 1. The core inlet subcooling was obtained from the process computer by performing an energy balance on the core downcomer.

The first operating date for which detailed benchmark data was recorded was April  $5^{th}$ , 1974. Core measurements were taken at 1" intervals for each of the 43 travelling in-core probe (TIP) positions. The measurements were condensed into 6" lengths by using a weighted average of 7 adjacent detector readings. Measurements taken at the boundary of each 6" node were applied to both surrounding nodes but given half weight in each. The end results are 24 measured points spaced 6" apart, for a total of 1032 points ( $24 \times 43$ ). In addition to the TIP data, each dataset consisted of a map of the control rod positions, the core exposure, the core thermal power, the steam dome pressure, the core flow, the core inlet subcooling. Data sets are extracted in roughly one month intervals and recorded in Table 2 for cycle 1. The cycle 2 data was also taken from the EPRI report but is not reproduced here because the power and flow are relatively constant across the entire cycle.

Table 2: Peach Bottom 2 Cycle 1 Data Sets

Datasat	Exposure	Power Thermal	Inlet Subcool	Core Flow	Dome Press
Dataset [MWd/MTU]		[MW]	[kJ/kg]	[kg/s]	[Pa]
1	253.53	1835	46.520	1.334E+04	7.136E+06
2	429.90	2603	43.496	1.360E+04	6.833E+06
3	714.30	2513	66.058	9.084E+03	6.943E+06
4	816.81	3164	51.405	1.357E+04	6.957E+06
5	1113.33	3261	53.033	1.331E+04	7.012E+06
6	1747.16	3280	59.778	1.223E+04	7.122E+06
7	2292.81	3292	55.359	1.299E+04	6.998E+06
8	2816.41	3265	56.754	1.275E+04	7.046E+06
9	3218.75	2856	72.571	9.916E+03	7.005E+06
10	3904.39	3271	56.057	1.308E+04	7.136E+06
11	4810.49	3280	55.591	1.312E+04	7.081E+06
12	5177.56	3277	55.591	1.310E+04	7.095E+06
13	5800.36	3293	56.289	1.299E+04	7.122E+06
14	6217.04	3283	54.428	1.337E+04	7.088E+06
15	6730.71	3215	53.265	1.337E+04	7.067E+06
16	7131.95	3172	53.033	1.328E+04	7.067E+06
17	7716.18	1649	69.082	6.312E+03	6.798E+06
18	8046.87	1855	96.529	5.027E+03	6.860E+06
19	8501.02	1882	97.925	5.090E+03	6.991E+06
20	8928.72	1858	95.133	5.153E+03	6.902E+06
21	9292.48	3285	51.172	1.349E+04	7.053E+06
22	9662.86	3292	57.220	1.275E+04	7.060E+06
23	10245.98	3255	51.405	1.344E+04	7.067E+06
24	11133.34	3001	57.452	1.366E+04	6.991E+06

### 3.1 PATHS Stand-alone Benchmarking

The PATHS solution is compared with TRACE in order to validate the methods developed in the previous section and evaluate the various void fraction models. First, equivalent TRACE and PATHS models are developed for an average single channel in the Peach Bottom 2 core. Three power shapes are applied to these models; uniform, sinusoidal, and bottom peaked. In addition to the nominal power and flow, cases are run at 1, 4, and 8 MW at 60%, 100%, and 140% of nominal flow. The power and flow perturbations are run with a sinusoidal power shape.

The three void fraction models are run for the twelve single channel cases and compared to the TRACE solution. The difference in the solution is quantified in two ways. The first is the algebraic mean of the difference between TRACE and PATHS. The second is the root mean square of the difference in the models. Table 3 summarizes the comparison between the three void fraction models. Both the EPRI void model and the GE-Ramp model show good comparisons with the TRACE solution, but the modified Bestion model shows a consistent under prediction of void for all cases.

Table 3: Difference In Void Fraction Models Compared with TRACE

The 14<sup>th</sup> International Topical Meeting on Nuclear Reactor Thermalhydraulics, NURETH-14 Toronto, Ontario, Canada, September 25-30, 2011

		Bestion	
Average	-1.21	0.33	1.76
RMS	1.68	1.65	3.15

The pressure drop is also compared in addition to the comparison of the void fraction. Pressure drops across BWR bundles is crucial to determine the radial flow distribution in the reactor. The different void fraction models give very comparable pressure drops across the channel. The comparison between the GE-Ramp model and TRACE are shown in Figure 1. The pressure drops compare very well at low and nominal flow rates. The largest pressure drops deviations are observed at high flow rates and low power which can be attributed primarily to differences in the thermo-physical properties.

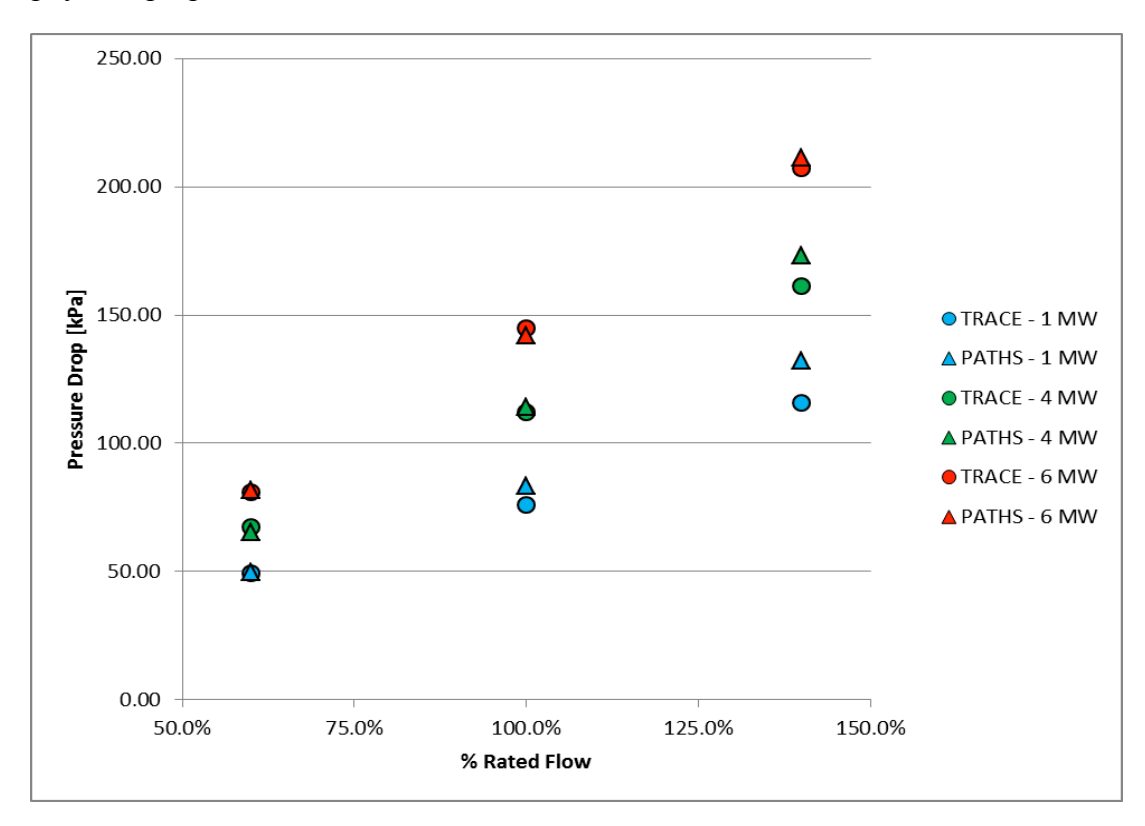


Figure 1: Pressure Drop Comparison between TRACE and PATHS

### 3.2 PATHS / PARCS Coupled Benchmarking

While the stand alone cases provide a good comparison of the different void models, a coupled neutronic and thermal fluids system must be solved to evaluate the impact of the void fraction models on practical power reactor problems. The Peach Bottom 2 OECD Turbine Trip Benchmark provides a steady state condition before the turbine trip. Cross-sections generated using CASMO-4 are provided along with the burnup and history information. Similar TRACE and PATHS models are defined with all 764 channels modelled separately. For simplicity, only the EPRI void fraction model is used in PATHS for the full core comparisons. A comparison between PATHS and TRACE predictions of the eigenvalue, nodal power peaking, and the overall execution time for the calculation is shown in Table 4 for this steady state condition.

Table 4: Peach Bottom Turbine Trip Steady State Comparison

	K <sub>eff</sub>	P <sub>xyz</sub>	P <sub>xy</sub>	P <sub>z</sub>	Runtime [sec]
TRACE/PARCS	1.00422	2.015	1.468	1.413	2307*
PATHS/PARCS:	1.00417	2.049	1.48	1.423	217

<sup>\*</sup>The TRACE/PARCS runtime is dependent on the time of the null transient because complex plant models are very difficult to converge. For these calculations, the null transient time is 300s.

The axial power shape is also worthwhile to analyze because TIP and LPRM (Local Power Range Monitor) data is available as an experimental verification of the models. The axial power shape for TRACE, PATHS, and the data is shown in Figure 2. The RMS difference in axial power shape between TRACE and PATHS is 1.82%.

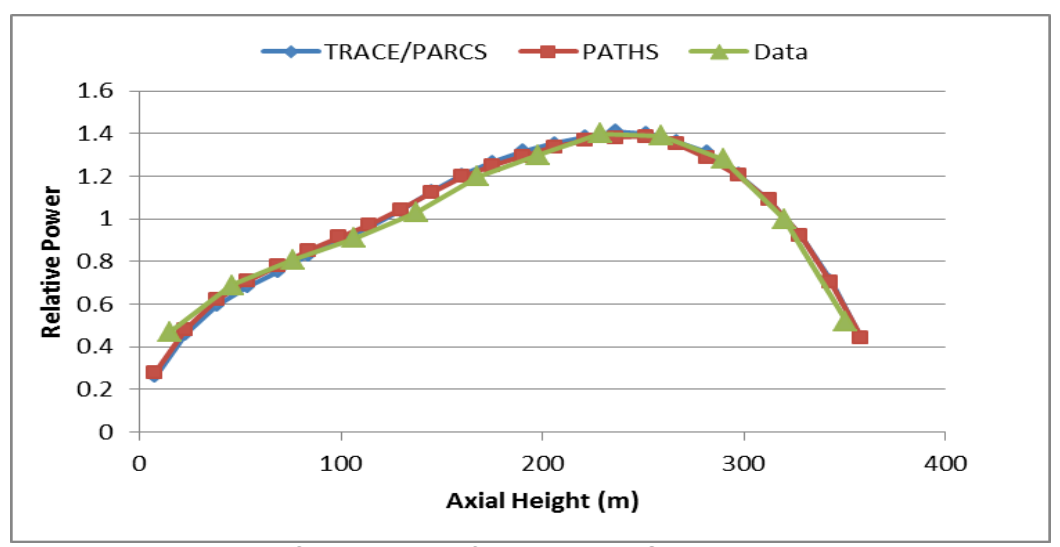


Figure 2: Comparison of Axial Power Shape with TIP Data

Another basis of comparison used here is the axially integrated radial power shape. The radial power distribution provides an indication of the accuracy of the core flow distribution. The RMS difference in the radial power shape between TRACE and PATHS is 0.8122%.

Finally, the LPRM data are compared to the LPRM predicted powers extracted from the PARCS/PATHS solution. Figure 3 shows the measured versus predicted LPRM powers where A, B, C, and D refers to the axial location of the LPRM from the bottom to the top of the core. As indicated in the figure, with the exception of a few points, there is generally reasonable agreement between the predicted and measured LPRM data.

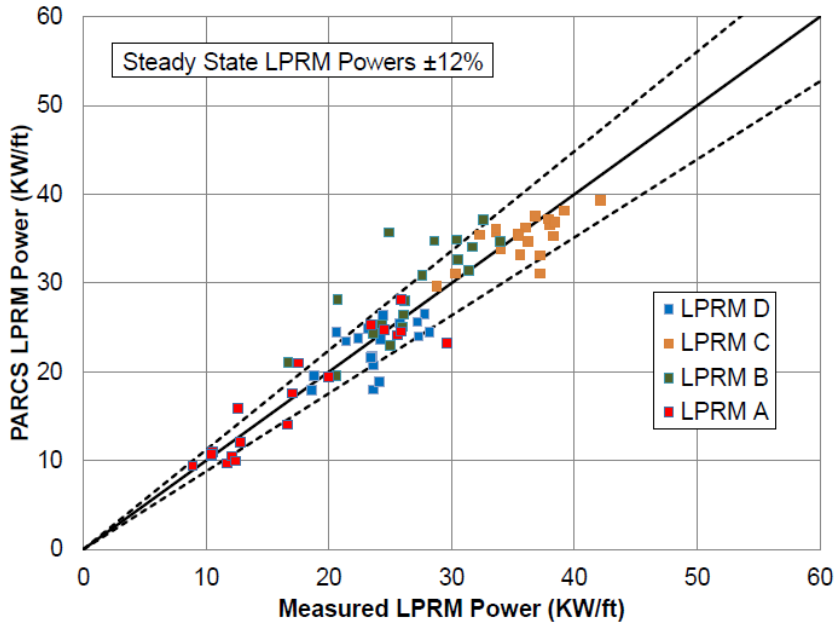


Figure 3: Measured vs. Predicted LPRM Power for PB2-TT1

## 3.3 PARCS / PATH Peach Bottom Depletion

The full core model was developed using PARCS with PATHS to follow the changes in power, flow, and control rod position during the depletion of cycles 1 and 2 of Peach Bottom. Figure 4 and 5 shows the eigenvalue trend for cycles 1 and 2, respectively, and Figure 5 shows a comparison of the TIP data at two state points in cycle 1 and 2.

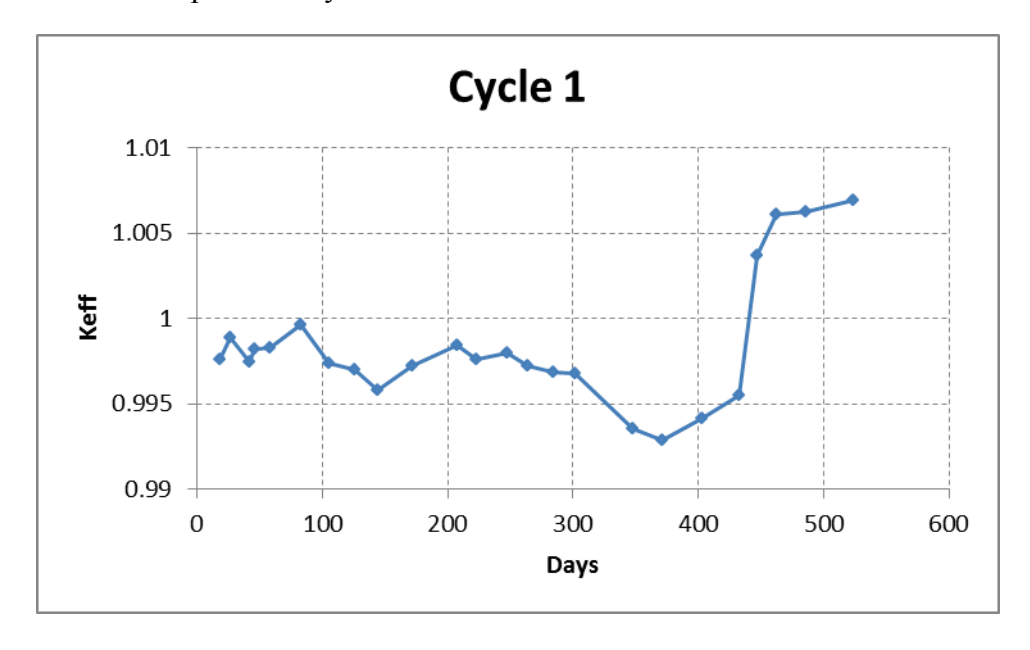


Figure 4: Peach Bottom Cycle 1 Depletion with PATHS

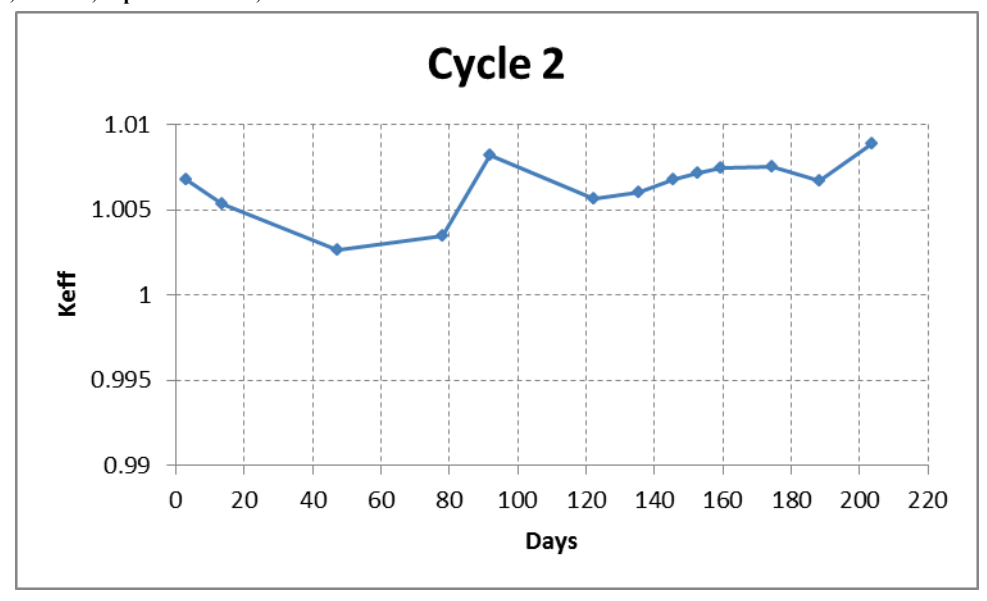


Figure 5: Peach Bottom Cycle 2 Depletion with PATHS

The accuracy of the prediction in the eigenvalue for both cycles is reasonable. There is a a noticeable increase in the eigenvalue prediction during cycle 1 which follows an extended period of at 50% power (see Table 2). The TIP comparisons shown in Figure 6 are at four different levels (Region 1-4) where Region 1 is the bottom of the core and Region 4 is the top of the core. Again, with the exception of certain locations in the core, there is a reasonable accuracy between the measured and predicted data that is not inconsistent with the reported for BWR depletion analysis within the industry [8].

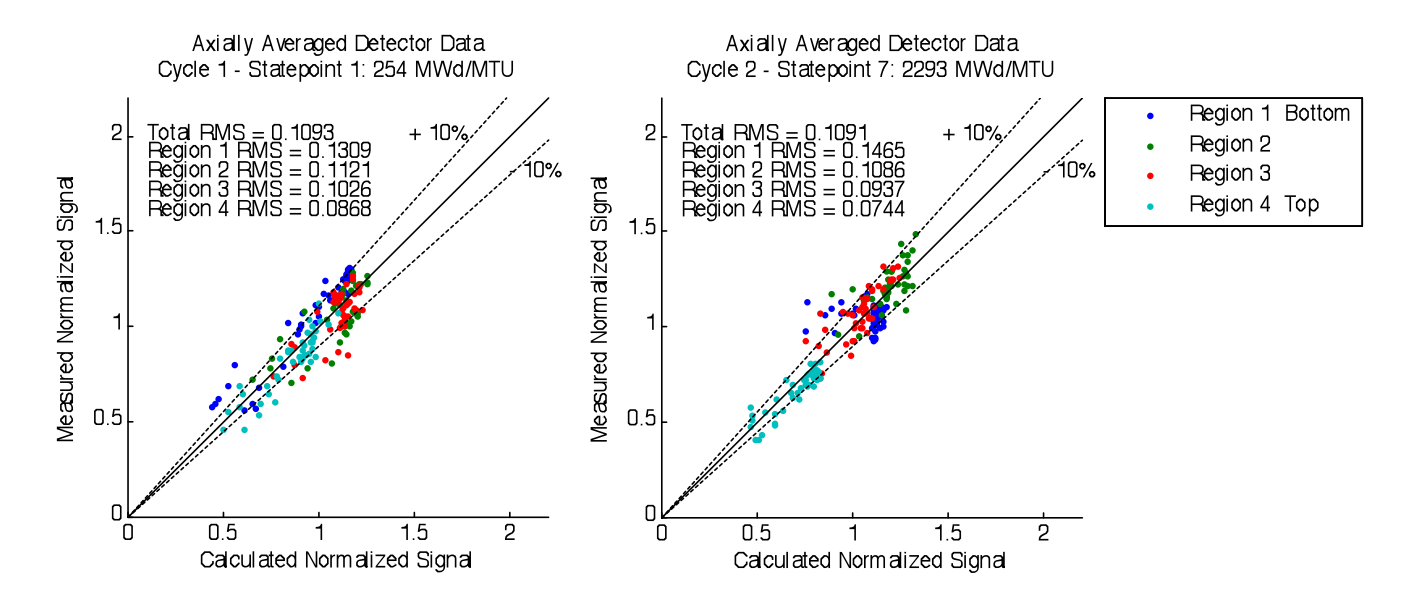


Figure 6: TIP Comparisons for Cycle 1 and Cycle 2 at BOC and MOC respectively

#### 4. Conclusion

The PATHS code has been developed to provide an internal two phase thermal hydraulic solver for the PARCS code to be used for BWR steady state and depletion calculations. The methodology is based on a three equation drift flux model that provides very efficient calculations with reasonable accuracy. The void fraction relationships implemented show good agreement with the TRACE code. The PARCS full core coupled code comparison shows that PATHS can be used the power shape accurately compared to TRACE and TIP data. Finally, cycle 1 and 2 of the Peach Bottom 2 reactor is simulated and comparisons are made with the measured power and flow conditions.

The development of PATHS and its implementation to provide a two-phase thermal-hydraulics steady-state solution enhances the functionality of PARCS for BWR depletion analysis. Work is continuing on development of the PATHS model to further improve the results for the Peach Bottom depletion and the validation base reported here is being extended to other BWRs.

# 5. Appendix A: List of Variables

и	Fluid mixture velocity
u*	Fluid mixture velocity from previous iteration
α	Void fraction
f	Friction Factor
$K_{loss}$	Loss Coefficient
$D_H$	Hydraulic Diameter
$\Phi_{2\Phi}$	Two Phase Friction Multiplier
h	Mixture enthalpy
$\Delta h_{fg}$	Specific Enthalpy of Vaporization
P	Mixture pressure
$P^*$	Mixture pressure from previous iteration
$q^{\prime\prime\prime}$	Volumetric Heat Generation
x	Steam Quality

## 6. Appendix B: Void Fraction Correlations

EPRI Void Model [9]

$$\kappa_1 = \min \left[ 0.8, \left( \frac{1}{1 + e^{-\frac{Re}{10^5}}} \right) \right] \qquad \kappa_o = \kappa_1 + \left( 1 - \kappa_1 \right) \left( \frac{\rho_g}{\rho_f} \right)^{0.2}$$

$$r = \frac{1 + 1.57 \left(\frac{\rho_g}{\rho_f}\right)}{1 - \kappa_1} \qquad C_1 = \frac{4P_c^2}{P(P_c - P)}$$

The 14<sup>th</sup> International Topical Meeting on Nuclear Reactor Thermalhydraulics, NURETH-14 Toronto, Ontario, Canada, September 25-30, 2011

$$\frac{1}{C_o} = \kappa_o + (1 - \kappa_o) \alpha^r \frac{1 - e^{-C_1}}{1 - e^{-C_1 \alpha}}$$

$$V_{gj} = \sqrt{2} \left( \frac{g \sigma \Delta \rho}{\rho_l^2} \right)^{1/4} \left( 1 - \alpha \right)^{3/2}$$

GE-Ramp [10]

$$C_{0} = \begin{cases} 1.1 & \alpha \leq 0.65 \\ 1 + 0.1 \frac{(1 - \alpha)}{0.35} & \alpha > 0.65 \end{cases}$$

$$V_{gj0} = \left(\frac{g\sigma\Delta\rho}{\rho_{l}^{2}}\right)^{\frac{1}{4}}$$

$$V_{gj} = \begin{cases} 2.9V_{gj0} & \alpha \leq 0.65 \\ 2.9\frac{(1 - \alpha)}{0.35}V_{gj0} & \alpha > 0.65 \end{cases}$$

Modified Bestion (Used in TRACE to determine interfacial drag) [1]

$$C_0 = 1.2 - 0.2 \sqrt{\frac{\rho_g}{\rho_l}}$$

$$V_{gj} = 0.188 \sqrt{\frac{g\Delta\rho D_h}{\rho_g}}$$

## 7. References

- [1] J. Spore *et al.*, LA-UR-00–910 TRAC-M/FORTRAN 90. Theory Manual, Los Alamos National Laboratory, Los Alamos, NM (2000).
- [2] K. Smith, et. al., 'SIMULATE-3 Methodology", Studsvik/SOA-95/18, (1995).
- [3] M. Ishii and T. Hibiki, Thermo-Fluid Dynamics of Two-Phase Flow, Springer, New-York (2006).
- [4] S.V. Patankar, Numerical Heat Transfer and Fluid Flow. McGraw-Hill, New York (1980).
- [5] W. Wagner, J.R. Cooper, and A. Dittmann, The IAPWS Industrial Formulation 1997 for the Thermodynamic Properties of Water and Steam. J. Eng. Gas Turbines Power. v. 122 (2000).
- [6] G. Lellouche and B. Zolotar, *Mechanistic Model for Predicting Two-Phase Void Fraction in Vertical Tubes, Channels, and Rod Bundles*, EPRI NP-2246-SR (1982).
- [7] "Core Design and Operating Data for Cycles 1 and 2 of Peach Bottom 2" EPRI NP-563, (1978).

The  $14^{\rm th}$  International Topical Meeting on Nuclear Reactor Thermalhydraulics, NURETH-14 Toronto, Ontario, Canada, September 25-30, 2011

- [8] A. Karve, et al, "Methods Comparisons for Hot Eigenvalue and TIP Predictions," ANS Winter Meeting, November 17-21, 2002, Washington, D.C.
- [9] B. Chexal and G.S. Lellouche, A Full-Range Drift-Flux Correlation for Vertical Flows. *EPRI-NP-3989-SR* (1986).
- [10] A. Manera, H. M. Prasser, and T.H.J.J. van der Hagen, "Suitability of Drift-Flux Models, Void Fraction Evolution and 3D Flow Pattern Visualization During Stationary and Transient Flashing Flow in a Vertical Pipe," Nuclear Technology. v. 152 (2005).